16

Alloying Effect in Low Loaded Rh Catalysts Supported on High Surface Area Alumina on Their Activity in CH_4 and NO Decomposition

Mieczysława Najbar** et al*
Faculty of Chemistry
Jagiellonian University
Poland

1. Introduction

1.1 The activity of Rh sites in Al-Rh alloys nanocrystallites in the reaction based on the electron transfer to the adsorbed molecules

In the alloys of transition metals (TM) and main group ones (MGM) the valence electrons from MGM can fill the d band of the TMs entirely and slightly increase the number of electrons in their s band (Azaroff, 1960; Kittel, 2005). Such Rh atoms enriched in electrons, present in Al-Rh alloys, were found to be very active electron donors (Pietraszek et al., 2007). It was revealed that they transfer the electrons to the antibonding Л orbital of adsorbed nitric oxide molecules causing NO decomposition to dinitrogen and dioxygen (Pietraszek et al., 2007).

Due to the great difference in the Al and Rh electro-negativity, the alloys are sometimes considered as nonstoichiometric chemical compounds. Because of the large range of nonstoichiometry those compounds should rather be estimated as intermediate phases (IP) (Azaroff, 1960).

The presence of the Al-Rh alloy nanocrystallites isostructural with Al_9Rh_2 (Bostrom et al., 2005) was earlier revealed in the freshly prepared $Rh/\delta Al_2O_3$ catalysts containing 0.06 and 1.5 wt.% Rh (Pietraszek et al., 2007; Zimowska et al., 2006).

It is well known that in bimetallic alloy crystallites (Gasser, 1985) the metal with the lower melting point segregates in their surface layers. The melting point of aluminum is much lower than that of rhodium (Lide, 2004-2005). The enrichment in aluminum of the surface of

* Patrick Da Costa[1], Jarosław Dutkiewicz[2], Valerio Choque[3], Narcis Homs[3], Paweł Kornelak[2], Agnieszka Pietraszek[2], Pilar Ramirez de la Piscina[3] and Janusz Sobczak[4]
[1]*The Jean le Rond d'Alembert Institute, University Pierre et Marie Curie, France*
[2]*Faculty of Chemistry, Jagiellonian University, Poland*
[3]*Department of Inorganic Chemistry, University of Barcelona, Spain*
[4]*Institute of Physical Chemistry PAS, Poland*
**Corresponding Author

the nanocrystallites of the Al-Rh intermediate phase at temperature 873K, close to Al melting point, should be very distinct.

The electron transfer from Rh atoms enriched in electrons to the antibonding orbitals of such molecules as O_2 and CH_4, leading to dissociation, can also be expected. The comparison of the enthalpy of the formation of NO, O_2 and CH_4 (Lide, 2004-2005) allows to expect the following sequence of the initial temperature of the dissociation: $T_{CH4} > T_{O2} > T_{NO}$.

Methane dissociation is the main step in one of the most intensively investigated process of the partial methane oxidation (PMO). Thus, it was interesting to compare the activity of the Rh active sites in the Al-Rh nanocrystallites which formed on the surface of the low-loaded Rh/Al_2O_3 catalysts with that of the Rh active sites in the rhodium clusters present on the surface of the high-loaded catalysts.

The study of the influence of the concentration of the atomic oxygen surface species on the Al-Rh alloy nanocrystallites on the composition of the PMO products is necessary to understand the role of the CH_4: O_2 ratio in the PMO process.

The investigations of the Al segregation in the Al-Rh alloy nanocrystallites allow one to understand the evolution of the surface structure during the catalyst use at temperatures higher than the synthesis temperature.

The simultaneous studies of the NO direct decomposition and CH_4 oxidation may confirm the expected sequence of the temperatures of the initial dissociation of CH_4, O_2 and NO. The knowledge of this sequence would help to estimate the temperature range of the effective direct NO decomposition in the off gases containing methane and an excess of oxygen.

1.2 The methane conversion in the oxygen presence to the synthesis gas over alumina supported rhodium catalysts

CO and H_2 mixture (the synthesis gas - syn-gas) is applied in the Fischer-Tropsch and methanol syntheses. Hydrogen for ammonia synthesis and the food industry is also obtained from the syn-gas.

At present the synthesis gas is produced mainly by the highly endothermic, and thus unfriendly for environment, methane steam reforming. The exothermic partial methane oxidation would be more economical and therefore more friendly for environment.

Since a C-H bond can be broken on Rh sites at relatively low temperatures (Wang et al., 1996), the endothermic methane dissociation to C atoms and dihydrogen, followed by carbon oxidation, is most frequently considered as a plausible mechanism of the partial methane oxidation to the synthesis gas over the Rh/Al_2O_3 catalysts (Enger et al., 2008; Hofstad et al., 1998; Mallens et al., 1997; Nakagawa et al., 1999; Wang et al., 1996). At PMO temperatures hydrogen practically does not adsorb on the Rh surface and thus the possibility of its interaction with surface oxygen or OH groups is rather low (Rieck & Bell, 1985).

The high price of rhodium limits the use of the high loaded Rh/Al_2O_3 catalysts. Therefore it is of interest to investigate the possibility of the use of the low-loaded ones in PMO. In such catalysts Al-Rh alloys can be formed, besides clusters of metallic Rh, as a result of the strong metal-support interaction (SIMS) (Pietraszek et al., 2007;Zimowska et al., 2006).

As it was discussed elsewhere (Zimowska et al., 2006), calcination of the precursors of the low loaded $Rh/\delta Al_2O_3$ catalysts (with the specific surface area ca $287 m^2/g$) causes Rh incorporation into the near-to-surface layers of the alumina nanocrystallites resulting in a Rh^{x+}/Al_2O_3 solid solution (Rh^{x+}/Al_2O_3 s.s.) formation. The reduction of such a s.s. leads to Al-Rh alloys.

1.3 The NO direct decomposition in the oxygen presence over alumina supported precious metal catalysts

Nitrogen oxides NO_x in the flue gases from fuel combustion contain more then 90% of NO. It is formed from air in the endothermic N_2 oxidation at temperatures above 1273K. NO is a thermodynamically unstable molecule with a high, positive formation enthalpy $\Delta H^o_{f\,(298)}$ = 90,2 kJ/mol. Therefore it could decompose to N_2 and O_2 at low temperatures (between 293 and 973K) (Chuang & Tan, 1997; Garin, 2001; Tonetto et al., 2003).

The NO decomposition seems to be the best way of NO removal from the flue gases of stationary sources of emission from a practical, environmental as well as an economical point of view. This process does not require any reducer that allows the avoidance of secondary pollutants like oxygenated hydrocarbons, CO, CO_2, NH_3 or even cyanate and isocyanate (Chuang & Tan, 1997; Parvulescu et al., 1998; Tonetto et al., 2003). However, in the case of the direct NO decomposition N_2O can be formed aside from N_2 in one of the two possible paths of the process (Parvulescu et al., 1998):

$$2NO \rightarrow N_2 + O_2 \quad (1)$$

$$2NO \rightarrow N_2O + \tfrac{1}{2}\, O_2 \quad (2)$$

Oxide supported Pt, Rh and Pd high-loaded catalysts are known to be the most active in the direct NO decomposition among the metal catalysts supported on metal oxides (Almusaiteer et al., 2000; Garin, 2001; Gorte et al., 1981; Ishii et al., 2002; Papp & Sabde, 2005; Pietraszek et al., 2007; Rahkamaa & Salmi, 1999; Root et al., 1983; Sugisawa et al., 2001; X. Wang et al., 2004). However, the NO dissociation proceeds on Rh active species in rhodium clusters with a satisfactory rate only above 623K and it is greatly suppressed by the oxygen presence. The reactive atomic species at such temperatures favor NO oxidation. On the other hand, the direct NO decomposition on the Rh active sites in Al-Rh alloy nanocrystallites (Pietraszek et al., 2007) formed on the low loaded alumina supported catalysts may proceed with a relatively high rate at 473K, below the temperature of the oxygen dissociation. The investigation of the alloying effect on the NO direct decomposition in the presence of oxygen and methane on a 0.18 wt.% $Rh/\delta Al_2O_3$ catalyst with rhodium present mostly in the Al-Rh nanocrystallites should give relevant information about the direct NO decomposition in off gasses formed during methane combustion.

2. Results and discussion

2.1 Experimental

Two 0.18 wt.% $Rh/\delta Al_2O_3$ catalysts were obtained by one- or three-step Rh^{3+} deposition on δ-alumina support. It was expected that such a procedure would produce catalysts with Rh sites of different coordination.

The structure of the Rh sites was determined by the FTIR spectroscopy of CO adsorbed and by XPS.

The δAl_2O_3 support ($287 m^2/g$) was obtained by the sol-gel method from aluminum tri-sec-butylate (Zimowska et al., 2006).

The one-step (1-S) and three-step (3-S) Rh depositions were performed from a $RhCl_3 \cdot 2H_2O$ aqueous solution of the same concentration.

The details of the Rh deposition as well as those of oxidising and reducing thermal treatments were described elsewhere (Pietraszek et al., 2007; Zimowska et al. 2006).

The first step of the 3-S synthesis of the 0.18 wt.% $Rh/\delta Al_2O_3$ catalyst consists of:

i/ the impregnation of the δAl_2O_3 support with the $RhCl_3 \cdot 2H_2O$ aqueous solution, ii/ the drying of a wet precursor, iii/ the calcination of a dry precursor at 773K and reduction at 623K and 773K of a calcined precursor. The used procedure yields the 0.06 wt.% $Rh/\delta Al_2O_3$ catalyst.

The next step of the 3-S synthesis of the 0.18wt.% $Rh/\delta Al_2O_3$ catalyst differs from the previous one only in the first stage; the 0.06 wt.% $Rh/\delta Al_2O_3$ catalyst (not the δAl_2O_3 support) is impregnated by the $RhCl_3 \cdot 2H_2O$ aqueous solution. As a result of the next drying, calcination and reduction the 0.12wt.%$Rh/\delta Al_2O_3$ catalyst is obtained.

In the third step of the 3-S synthesis the 0.12 wt.% $Rh/\delta Al_2O_3$ catalyst is impregnated by the same $RhCl_3 \cdot 2H_2O$ aqueous solution. The next drying, calcinations and reduction yields the 0.18 wt. % $Rh/\delta Al_2O_3$ catalyst.

The 1-S synthesis of the 0.18 wt.% $Rh/\delta Al_2O_3$ catalyst consists of: i/ the impregnation of the δAl_2O_3 support with a triple portion of the $RhCl_3 \cdot 2H_2O$ aqueous solution, ii/ the drying of a wet precursor, iii/ the calcination of a dry precursor and the reduction of a calcined precursor.

The FTIR spectroscopy of CO adsorbed and XPS measurements were performed for the fresh one-step (F-1-S) and three-step (F-3-S) catalysts as well as for the one-step and three-step catalysts subjected to the interaction with six methane pulses (U-1-S) and (U-3-S).

CO was adsorbed on the surface of the catalysts at room temperature and the spectra were taken also at room temperature after outgasing at 373K using a Nicolet 5700 Nexus spectrometer at a resolution of 4 cm^{-1}.

The XPS measurements for F-1-S, F-3-S, U-1-S, and U-3-S catalysts were carried out using a scanning photoelectron spectrometer PHI 5000 VersaProbe (Physical Electronics USA/ULVAC Japan) with monochromatic Al Kα radiation (1486.6eV). The signal was collected from 200 x200μm area using an x-ray beam focused to 100μm diameter with 25 W power. For the charge shift compensation all the measurements were made with neutralization by low energy electrons and argon ions. The survey spectra were obtained with a pass energy of 117.4eV in 0.4eV increments. The detailed spectra of the Rh3d, and the Al2p regions were measured with a pass energy of 23.5eV in 0.1eV increments. The binding energy scale (BE) was calibrated based on the Al2p in a Al_2O_3 support signal (BE = 74.3eV). Signal components were fitted using a non-linear least squares fitting Casa XPS software. The quantitative analysis was done after a Shirley-type background subtraction using the Scofield sensitivity factors.

The investigation of the interaction of the catalysts with methane pulses was carried out at 873K in an acid-resistant steel tubular reactor with a 6mm internal diameter and 30cm length, under the pressure of 280 kPa and at GHSV =9000h^{-1}. The 700 mm^3 methane pulses were introduced into the Ar stream flowing through the reactor, the Carboxen 1000 packed column and the TCD detector of a Hewlett-Packard 5890 chromatograph. The time between consecutive methane pulses was ca. 32min.

The direct NO decomposition in methane and the oxygen presence was investigated under the steady-state conditions in 473-673K temperature range. The reaction mixture of 150ppm NO 1500ppm CH_4, 7%O_2 and Ar as a balance passed over the catalyst placed on quartz-wool in a quartz reactor with GHSV = 20 000h^{-1}. Before the steady-state experiment the catalyst was heated in the reaction mixture from the r.t. to 773K and consecutive measurements were performed stepwise starting from 673K to 473K. A FID detector was used to follow the total concentration of hydrocarbons and the N_2 formation was checked by a micro-GC.

2.2 The physicochemical characterisation of 0.18wt.%Rh/δAl_2O_3 catalysts by FTIR spectroscopy of CO adsorbed and XPS

Fig. 1. presents the FTIR spectra of CO adsorbed on the F-3-S 0.18wt.%Rh/δAl_2O_3 catalyst (a) and on the F-3-S 0.18 wt.% Rh/δAl_2O_3 one (b). In agreement with the data extensively reported in the literature (Finocchio et al., 2007 ; Hadjiivanov &Vayssilov, 2002; Kraus et al., 1989; Lavalley et al., 1990; Paul et al., 1999; Yates et al., 1979) two main bands at 2087 and 2013 cm^{-1}, present in the spectra of both the catalysts, can be assigned to symmetric and asymmetric stretching vibrations of gem-bicarbonyls adsorbed on the Rh atomically dispersed

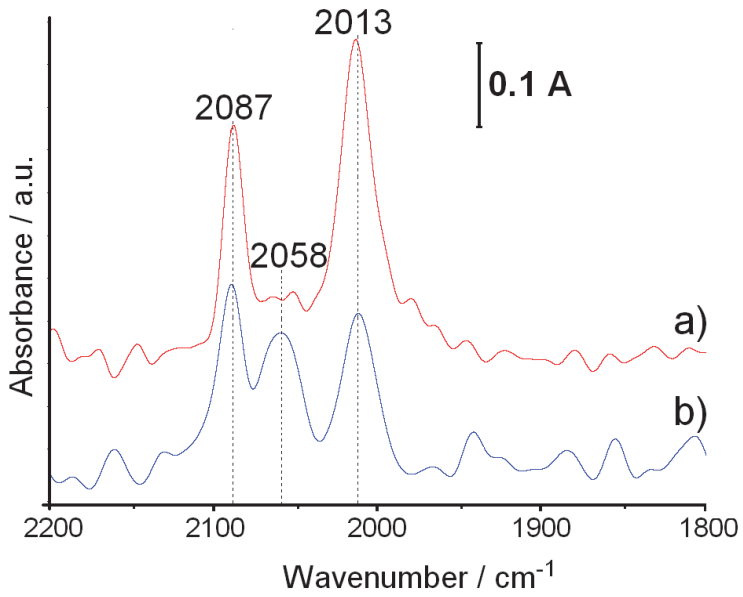

Fig. 1. DRIFT spectra CO adsorbed on the surface of the 0.18 wt.% Rh /δAl_2O_3 catalysts obtained by: a/three-step rhodium deposition, b/ one-step rhodium deposition

on the alumina surface. However, the exact position of the atomically dispersed Rh in the structure of catalyst has yet to be determined (Finocchio et al., 2007 ; Hadjiivanov &Vayssilov, 2002; Kraus et al., 1989; Lavalley et al., 1990; Paul et al., 1999; Yates et al., 1979). According to above cited papers the peak at 2058cm^{-1}, clearly seen in the spectrum of the F-1-S catalyst, results from C-O stretching vibrations in CO linearly adsorbed on the Rh clusters.

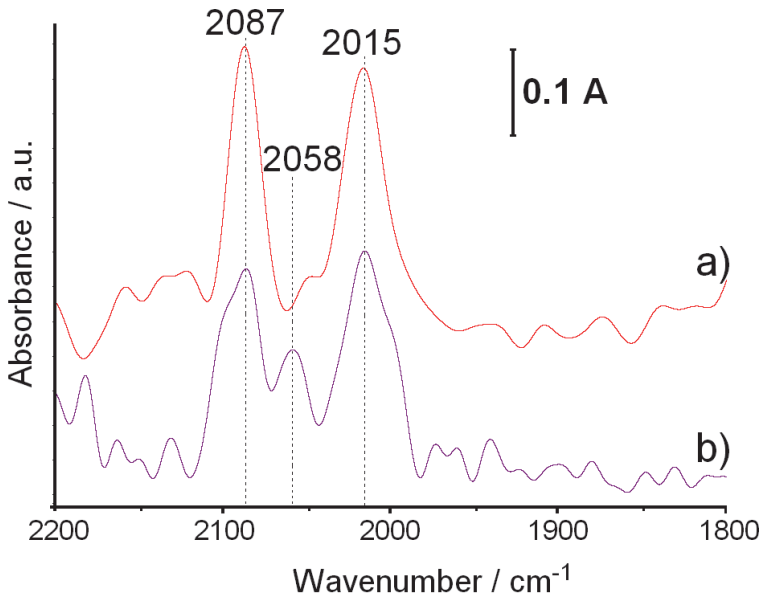

Fig. 2. DRIFT spectra of CO adsorbed on the surface of the 0.18 wt.% Rh /δAl_2O_3 catalysts: a/ obtained by a three-step rhodium deposition and subjected to interaction with six methane pulses, b/ obtained by a one-step rhodium deposition and subjected to interaction with six methane pulses.

Thus one may conclude that on the surface of the F-1-S catalysts the atomically dispersed Rh coexists with the Rh clusters. However, on the surface of the F-3-S catalyst atomically dispersed species are hardly seen.

Fig. 2 presents the FTIR spectra of CO adsorbed on the three-step (a) and one-step (b) 0.18wt.% Rh/δAl_2O_3 catalysts subjected to interaction with 6 methane pulses at 873K.

The distinct decrease of the ratio of Rh in clusters to Rh in alloy nanocrystallites as a result of the catalysts interaction with methane pulses is observed. The increase of the width of the gem-bicarbonyl peaks reveals that during the pulse experiment atomically dispersed Rh with a coordination slightly different than in the fresh catalysts is formed.

The comparison of XPS results for the fresh and used catalysts gives further insight in the nature of atomically dispersed rhodium species and in the mechanism of their creation as well as their interaction with the clustered metallic rhodium species.

In Table 1 the BEs of peaks obtained by the deconvolution of the $Al2p_{3/2}$ and $Rh3d_{5/2}$ bands as well as the percentage of the particular Al and Rh species ($(Me^x/\Sigma Rh^x+\Sigma Al^x)\cdot 100$) in F-1-S, U-1-S, F-3-S and U-3-S catalysts are presented.

Catalyst	Peak	BE [eV]	$(Me^x/\Sigma Rh^x+\Sigma Al^x)\cdot 100$ [at.%]*
F-1-S	$Rh3d_{5/2}$	310.0	0.08
		307.4	0.05
	$Al2p_{3/2}$	74.3	99.87
U-1-S	$Rh3d_{5/2}$	307.5	0.003
		305.0	0.003
	$Al2p_{3/2}$	75.4	15.69
		74.3	84.30
F- 3-S	$Rh3d_{5/2}$	310.2	0.06
		307.8	0.09
	$Al2p_{3/2}$	75.5	9.72
		74.3	90.13
U- 3-S	$Rh3d_{5/2}$	309.6	0.003
		307.2	0.003
	$Al2p_{3/2}$	75.4	14.21
		74.3	85.70

M^x – metallic or cationic Rh and/or Al species

Table 1. The XPS results for the fresh one-step (F-1-S) and the three-step (F-3-S) 0.18 wt.% Rh/ δ Al_2O_3 catalysts and for those catalysts subjected to the interaction with six methane pulses (U-1-S and U-3-S).

The $Al2p_{3/2}$ bands in the spectra of the particular catalysts were deconvoluted into two peaks. The major peaks were ascribed to Al in alumina - BE=74.3eV (Wagner et al., 2007).

The BE of the less intensive $Al2p_{3/2}$ peaks as well as those of the Rh $3d_{5/2}$ peaks were determined with respect to this one. The less intensive $Al2p_{3/2}$ peaks with exceptionally high BE (75.4-75.5eV) were ascribed to Al in the Al-Rh alloy. The transfer of the valence Al electrons mainly to Rh unoccupied d-orbitals (Azaroff, 1960; Kittel, 2005) in the alloy should cause the increase of the $Al2p_{3/2}$ BE and decrease of $Rh3d_{5/2}$ one with respect to those in separate metals (Wagner, 2007).

The $Rh3d_{5/2}$ bands in the XPS spectra of the F-1-S and F-3-S catalysts were deconvoluted into the peaks of cationic species with BE equal to 310.0 and 310.2eV and of Al-Rh alloy ones with BE equal to 307.4 and 307.8 eV, a little lower than that of metallic Rh (Wagner, 2007).

The atomically dispersed Rh species (Finocchio et al., 2007; Hadjiivanov &Vayssilov, 2002; Kraus et al., 1989; Lavalley et al., 1990; Paul et al., 1999; Yates et al., 1979) demonstraded in the FTIR spectra of CO adsorbed on the F-1-S and the F-3-S catalysts (Fig.1) by bands at 2087 and 2013 cm^{-1}, occur probably in the surface lattice position of the Al-Rh alloy nanocrystallites.

The presence of only one $3d_{5/2}$ peak of the Rh species with BE =307.4 eV in the spectrum of the F-1-S catalyst reveals an electronic interaction between the Al-Rh intermediate phase nanocrystallites and the Rh clusters. It shows that the Rh clusters occur in the immediate proximity of the Al-Rh nanocrystallites. Such an electronic interaction was earlier observed by Thiam et al. (Thiam et al., 2004) between aluminum foil and a rhodium overlayer.

A higher percentage of the metallic Rh species in the F-3-S catalyst (60 %) than in the F-1-S one (ca 40%) could easily be explained by the differences in the syntheses. The one-step Rh deposition is thought to have occurred preferably on the smallest nanocrystallites with the highest surface/bulk ratio, possibly by an Rh^{3+} cation exchange with protons of the accessible acidic OH groups on alumina. Thus, the Rh deposition calculated per volume unit of alumina crystallites is higher the smaller their dimensions are. Rhodium clusters are formed from an excess of the aqueous Rh^{3+} ions solution present in pores.

On the other hand, the three-step Rh deposition occurs mostly by exchange of the Rh cations with the acidic OH group protons on the surface of the smallest δ alumina crystallites, which is renovated in each synthesis step in the course of the calcinations. It results in the exceptional enrichment of these crystallites in Rh. An incorporation of rhodium into δ alumina during the thermal treatments causes the formation of the Rh^{x+}/Al_2O_3 solid solution. The reduction of the s.s. nanocrystallites, resulting in inter-metallic Al-Rh alloy formation, is easier the higher the rhodium concentration is.

It is obvious that the enrichment of Rh atoms in electrons is the greater the higher their dispersion is in the aluminium matrix. Earlier this problem in particular was discussed regarding the Cu-Ni alloys (Kittel, 2005).

The interaction of the F-1-S catalyst with six CH_4 pulses causes a complete disappearance of the cationic Rh species and a great decrease in the content of the metallic Rh species. Simultaneously the Rh species with $3d_{5/2}$ BE equal to 305.0 eV and the Al species with an exceptionally high $2p_{3/2}$ BE (75.4eV) do appear.

The disappearance of the cationic species reveals the formation of the new nanocystallites of the Al-Rh alloy by the reduction of the Rh^{x+}/Al_2O_3 s.s. of low Rh content.

The major decrease of the content of Rh species with $3d_{5/2}$ BE close to 307 eV and the appearance of the species with $3d_{5/2}$ BE = 305 eV and the Al ones with $2p_{3/2}$ BE = 75.4 eV could be the result of the Al surface segregation in the alloy nanocrystallites formed at 773K. However, Rh species with $3d_{5/2}$ BE = 305 eV and the Al ones with $2p_{3/2}$ BE = 75.4 eV could also be formed as a result of the reduction of the Rh^{x+}/Al_2O_3 s.s. with a low Rh content.

The heating of the F-3-S catalyst and its interaction with 6 methane pulses causes a great decrease in the total contents of the Rh species in the surface nanolayers, the disappearance of the species with $3d_{5/2}$ BE = 307.8 eV, the appearance of the ones with $3d_{5/2}$ BE = 307.2 eV and an increase of the content Al species with $2p_{3/2}$ BE = 75.4 eV.

The major decrease in the content of the cationic and metallic Rh species, the the decrease in the $3d_{5/2}$ BE of the Rh metallic species as well as the increase of the content of the Al ones with $2p_{3/2}$ BE = 75.4 eV reveal the reduction of the Rh/Al_2O_3 s.s. areas with a small Rh content and Al segregation in the Al-Rh alloy nanocrystallites formed at 773K. The great extent of the surface Al segregation can be caused by great difference in Al and Rh melting points and the proximity of the used temperature and the temperature of Al melting (Lide, 2004-2005).

2.3 Methane dissociation on 1-S and 3-S 0.18 wt.% $Rh/\delta Al_2O_3$ catalysts

In Fig 3. the methane conversion (C_{CH4}), selectivity to hydrogen (S_{H2}), selectivity to CO (S_{CO}) and selectivity to CO_2 (S_{CO2}) in six consecutive CH_4 pulses over F-1-S catalyst are presented.

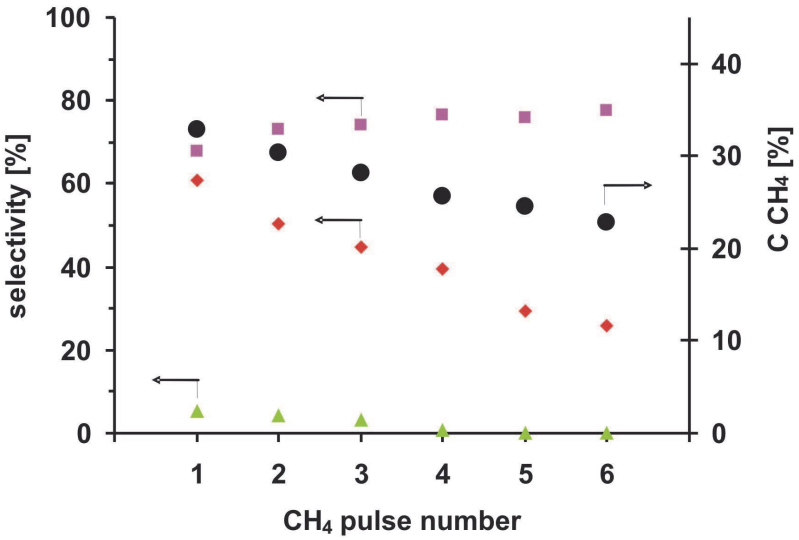

Fig. 3. CH_4 conversion (●) and selectivity to H_2(■), CO (♦) and CO_2 (▲) in six consecutive CH_4 pulses over the one-step 0.18 wt.% $Rh/\delta Al_2O_3$ catalyst (873K, 280kPa, 9000 h^{-1}).

The CH_4 conversion in the first pulse over the 1-S catalyst is equal to 33%, the selectivity to H_2 – 68%, the selectivity to CO - 61% and to CO_2 – 10%. In the following methane pulses C_{CH4} continuously decreases down to 23% in the sixth pulse. The S_{H2} increases up to 78 % in the sixth pulse, S_{CO} decreases, almost linearly, down to 22% in the sixth pulse and the S_{CO2} drops to 0% in the fourth pulse.

The simultaneous decrease of the C_{CH4}, the S_{CO} and the S_{CO2} and the increase of S_{H2} in the consecutive methane pulses can be explain by the decreasing concentration of the atomic species of oxygen adsorbed on the surface Rh species in Al-Rh alloy nanocrystallites and in Rh clusters present on the surface of the 1-S catalyst.

The initial S_{H2} increase accompanied by a decrease in S_{CO2} reveals that further formation of alloy nanocrystallites with a low concentration of Rh sites have a greater ability to transfer electrons to methane molecules. The 2.8 fold decrease in the S_{CO} in the sixth methane pulse with respect to that in the first methane pulse with a simultaneous increase of the selectivity to hydrogen, suggesting deeper methane dissociation, clearly shows a carbon deposition on the catalyst surface as a result of the deficit of oxygen species adsorbed.

In Fig. 4 the methane conversion, selectivity to hydrogen, selectivity to CO and the selectivity to CO_2 in six consecutive CH_4 pulses introduced to the reactor containing the F-3-S catalyst are presented.

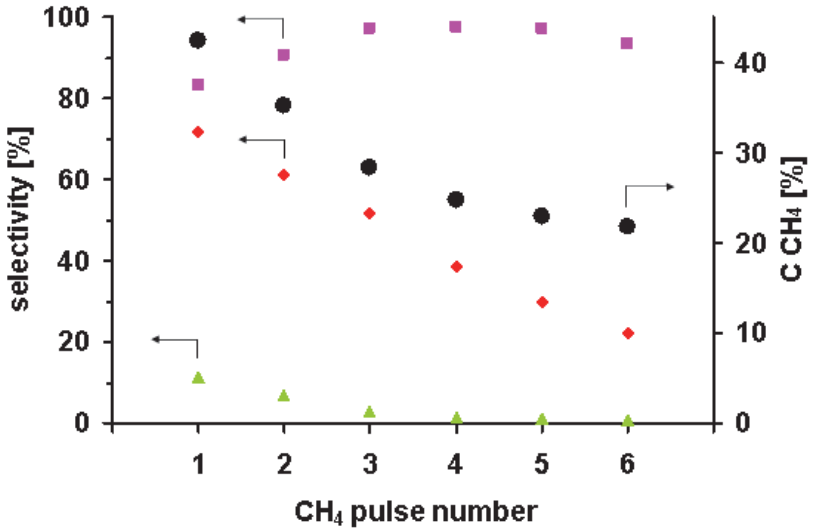

Fig. 4. CH_4 conversion (●) and selectivity to H_2(■), CO (♦) and CO_2 (▲) in six consecutive CH_4 pulses over the 3-S 0.18wt.% Rh/δAl_2O_3 catalyst (873K, 280kPa, 9000 h^{-1}).

The C_{CH4} in the first methane pulse is equal to 42%, the S_{H2} - 83%, the S_{CO} - 72% and the S_{CO2} – 11%. In the next methane pulses the C_{CH4} decreases down to 22% in the sixth pulse. The S_{H2} increases up to 98% in the third pulse and slowly decreases to 94% in the sixth pulse. The S_{CO} decreases almost linearly down to 22% in the sixth pulse and S_{CO2} drops to 0% in the fourth pulse.

The simultaneous decrease in the S_{CO2} and increase of the S_{H2} in the consecutive methane pulses up to the forth one could be ascribed to the formation of the new Al-Rh alloy nanocrystallites of a low content of Rh sites with a great ability to transfer the electrons to the methane molecules adsorbed.

There is a 50% decrease in the C_{CH4} and approximately a 70% decrease in the S_{CO} in the sixth pulse in comparison with the first one, not accompanied by the decrease in the S_{H2} which reveals carbon deposition on the Al-Rh alloy nanocrystallites.

The formation of the new alloy nanocrystallites by the reduction of the Rh/Al_2O_3 s.s. of the relatively low rhodium concentration causes the creation of a very active Rh species.

The stronger S_{CO} decrease on the 3-S catalyst (3.3 fold) of a higher activity than on the 1-S one (2.8 fold) of lower activity reveals that carbon is preferably deposited on the Al-Rh nanocrystallites.

The higher conversion of the first methane pulse over the F-3-S catalyst than over the F-1-S reveals that the Rh active species in the Al-Rh alloy nanocrystallites are more active in the methane dissociation than those in the Rh clusters (Figs.1 and 2). The decrease of the activity of both the catalysts in the consecutive pulses corresponds to the decrease of the total content of the Rh species accessible for methane adsorption.

The slower the decrease of the methane conversion over the 1-S catalyst than that over the 3-S one may be assigned to a slower carbon deposition on the Rh clusters than on the Al-Rh nanocrystallites.

On the other hand, the higher selectivity to hydrogen over the 3-S catalyst than over the 1-S one clearly shows a beneficial influence of the Al proximity on the Rh sites ability to transfer electrons to antibonding orbitals of methane.

Fig. 5 presents CH_4 conversion and selectivity to H_2, CO and CO_2 in 41 consecutive CH_4 pulses over the 3-S 0.18wt.% $Rh/\delta Al_2O_3$ catalyst (873K, 280kPa, 9000 h^{-1}). The methane pulses were introduced into the reactor mostly in time intervals close to 30min. Less regular time intervals (30-37min.) were applied between the 11th and 17th pulses as well as the 25th and 33rd. The C_{CH4} and S_{CO} decrease and S_{H2} increases in consecutive pulses up to the pulse 11. Irregular intervals between the 11 - 17 pulses and the 25 – 33 ones cause fluctuations in the C_{CH4}, the S_{CO} and the S_{H2} that can be ascribed to the changes in the amount of the carbon deposit oxidized by the oxygen from the gas phase. The 75 min. time interval between 34th and 35th pulses resulted in the C_{CH4} increase of 11% and of the S_{CO} of 110%. The increase of the time between the 40 and 41 pulses to 110 min. results in the increase of the C_{CH4} of 25% and of the S_{CO} of 230%. However, the selectivity to hydrogen does not change distinctly in any case. Thus, one can conclude that a long term interaction of the surface of the Al-Rh nanocrystallites, containing the carbon deposit, with the gas phase containing traces of oxygen causes both a carbon deposit removal by oxidation and oxygen adsorption. The oxidation of the carbon deposit causes the recovery of the Rh sites active in the methane dissociation that results in the increase of the C_{CH4}. The surface oxygen species cause oxidation of the carbon formed due to methane dissociation, that leads to the S_{CO} increase. However, their population is not high enough to have an effect on the S_{H2}. Thus, to perform the PMO with the high methane conversion and the high selectivity to CO and H_2 the proper CH_4:O_2 ratio is needed.

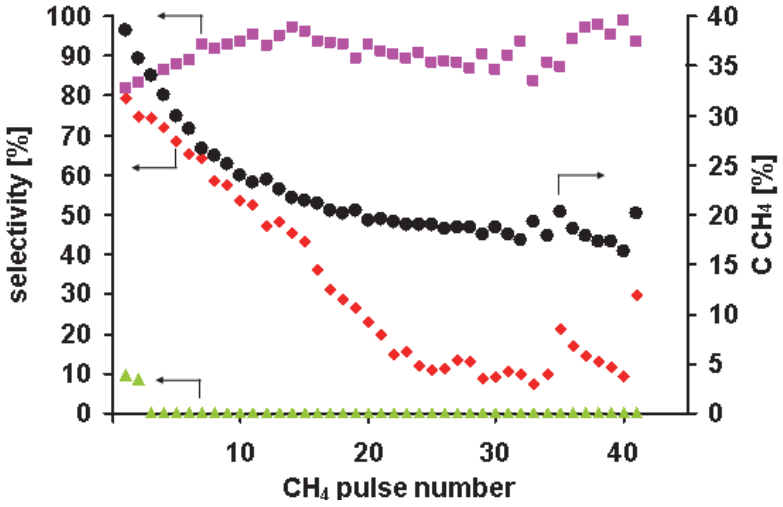

Fig. 5. CH_4 conversion (●) and selectivity to H_2(■), CO (♦) and CO_2 (▲) in 41 consecutive CH_4 pulses over the 3-S 0.18wt.% $Rh/\delta Al_2O_3$ catalyst (873K, 280kPa, 9000 h^{-1}).

2.4 Direct NO decomposition over the three-step (3-S) 0.18 wt.% Rh/δAl_2O_3 catalyst

NO conversion (C_{NO}), selectivity to N_2 (S_{N2}) calculated from the results of the steady-state experiments over the 3-S 0.18wt.%Rh/Al_2O_3 catalysts, are presented in Figure 6.

The steady-state experiment was performed with the use of the reaction gas containing 150ppm NO, 1500ppm CH_4, 7%O_2 and Ar as a balance.

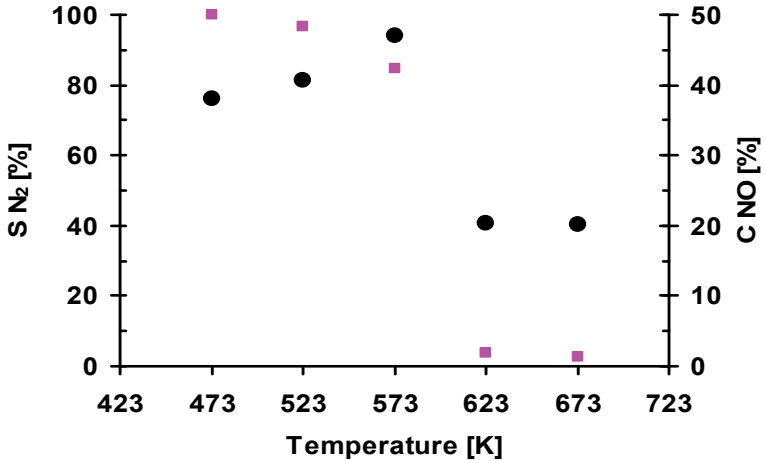

Fig. 6. NO conversion (●) and selectivity to NO (■) over three-step a 0.18 wt.% Rh/δAl_2O_3 catalyst (150ppmNO +1500ppm CH_4 + 7%O_2 /He , 20000h^{-1}, data from steady-state experiment)

The highest NO conversion, increasing with a temperature increase, from 38 to 47%, is observed at a temperature range 473K - 573K. The highest but decreasing from 100% to 85% selectivity to N_2 is achieved in the same temperature. A simultaneous sudden drop of the S_{N2} and a deep decrease in C_{NO} are observed at 623K.

The direct NO decomposition over the high-loaded rhodium catalysts supported on alumina was earlier observed only at temperatures higher than 623K (Garin, 2001).

Thus, the low-temperature NO decomposition on the low loaded 0.18wt.%Rh/δAl_2O_3 catalyst confirms exceptional activity of the Rh sites in Al-Rh alloy.

A simultaneous increase of the C_{NO} and the decrease of the S_{N2} with the temperature increase in the 473K - 573K range could be explained by the competitive dissociative O_2 adsorption on the Rh active sites, increasing with temperature. The atomic oxygen species block the Rh sites active in the direct NO decomposition and facilitate the NO oxidation.

The simultaneous sudden drop of the S_{N2} and a great decrease in the C_{NO} at 623K shows that blocking the Rh sites-active in the NO dissociation becomes much stronger. Such blocking may originate in a methane dissociation on the same sites. In Fig. 7, the CH_4 conversion (C_{CH4}) and selectivity to CO_2 (S_{CO2}), measured during the thermo-programmed catalyst heating at the rate of 3K/min in the reaction mixture containing 150ppm NO, 1500ppm CH_4, 7%O_2 and Ar as a balance, are presented.

The temperature of the sudden drop of the S_{N2} and C_{NO} (Fig. 6) corresponds to the initial temperature of the total methane oxidation to CO_2 (Fig. 7). This confirms competitive methane adsorption on the Rh active sites leading to the formation of the carbon species undergoing oxidation to CO_2.

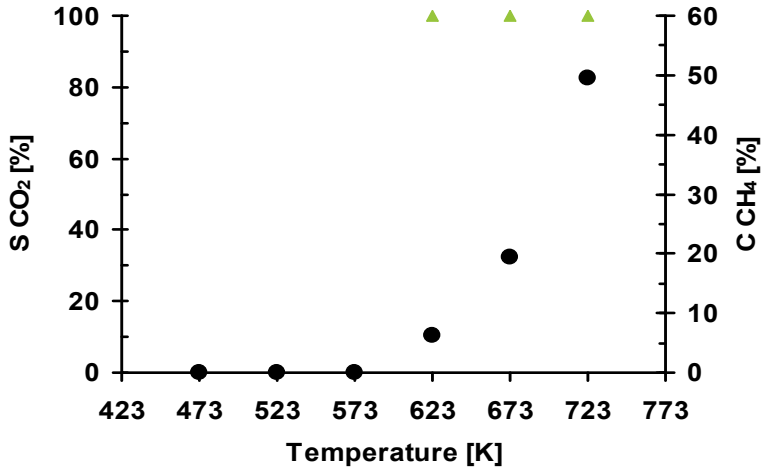

Fig. 7. CH_4 conversion (●) and selectivity to CO_2 (▲) over three-step 0.18 wt.% $Rh/\delta Al_2O_3$ catalyst (150ppmNO +1500ppm CH_4 + 7%O_2 /He , 20000h^{-1}, data from TPSR experiment)

3. Conclusions

The DRIFT spectroscopy of the adsorbed CO and XPS were used to show the formation of the Al-Rh alloy nanocrystallites on the surface of the 0.18 wt % $Rh/\delta Al_2O_3$ catalysts obtained by the one-step or three-step impregnation of the high surface area alumina support with the $RhCl_3$ aqueous solution (1-S and 3-S catalysts).

The effect of Al-Rh alloying on the catalyst activity in the methane dissociation and the direct NO decomposition was investigated.

The activity and selectivity to dihydrogen and to carbon monooxide of both the catalysts were determined at 873K. The results showed unambiguously that alloying distinctly enhances the Rh site activity in the electron donation to antibonding orbitals of methane molecules adsorbed. The observed enhancement of the Rh site activity was ascribed to the Al valence electrons transfer to the Rh 4d shell and slightly to the Rh 5s shell. The direct NO decomposition in the presence of oxygen and methane was investigated in the temperature range of 673-473K over a 3-S catalyst. The NO conversion with 100% selectivity to dinitrogen on the Rh active sites was revealed at an unexpectedly low temperature (473K). Simultaneous increase of the activity and decrease in the selectivity to dinitrogen with a temperature increase up to 573K clearly revealed a competitive dissociative oxygen adsorption on the same active sites. However, the sudden decrease at 623K of the catalyst activity in the NO decomposition and the selectivity to dinitrogen, accompanied by an initial methane oxidation to CO_2, undoubtedly showed competitive methane dissociation.

4. Acknowledgment

The polish authors (M. N, J. D. and P. K.) acknowledge the financial support by the European Regional Development Fund under the Innovate Economy Operational Programme 2007-2013, POIG.01.01.02-12-112/09 project.

5. References

Almusaiteer, K.; Krishnamurthy, R. & Chuang, S.S.C. (2000). In situ infrared study of catalytic decomposition of NO on carbon-supported Rh and Pd catalysts. *Catalysis Today*, Vol.55, No.3, pp. 291-299, ISSN 0920-5861

Azaroff, L.V. (1960). *Introduction to Solids*, McGRAW-Hill Book Cmpany, New York

Bostrom, M.; Rosner, H.; Prots, Y.; Burkhardt, U. & Grin,Y. (2005). The Co_2Al_9 Structure Type Revisited. *Zeitschrift für anorganische und allgemeine Chemie,*Vol.631, No.2-3, pp.534-541, ISSN 1521-3749

Chuang, S.S.C. & Tan, C.–D. (1997). Promotion of oxygen desorption to enhance direct NO decomposition over Tb−Pt/Al_2O_3 catalyst. *The Journal of Physical Chemistry B*, Vol.101, No.15, pp. 3000-3004, ISSN 1520-5207

Enger, B.C.; Lodeng, R. & Holmen, A. (2008). A review of catalytic partial oxidation of methane to synthesis gas with emphasis on reaction mechanisms over transition metal catalysts. *Applied Catalysis A: General*, Vol.346, No.1-2, pp.1-27, ISSN 0926-860X

Finocchio, E.; Busca, G.; Forzatti, P.; Groppi, G. & Beretta, A. (2007). State of supported rhodium nanoparticles for methane catalytic partial oxidation (CPO): FT-IR studies. *Langmuir*, Vol.23, No.20, pp. 10419–10428, ISSN 1520-5827

Garin, F. (2001). Mechanism of NO_x decomposition. *Applied Catalysis A: General,* Vol.222, No.1-2, pp. 183-219, ISSN 0926-860X

Gasser, R.P.H. (1985). An introduction to chemisorption and catalysis by metals, Oxford University Press, ISBN 0-19-855163-0, New York

Gorte, R.J.; Schmidt, L.D. & Gland, J. L. (1981). Binding states and decomposition of NO on single crystal planes of Pt. *Surface Science*, Vol.109, No.2, pp. 367-380, ISSN 0039-6028

Hadjiivanov, K.I. & Vayssilov, G.N. (2002). Characterization of oxide surfaces and zeolites by carbon monoxide as an IR probe molecule. *Advances in Catalysis*, Vol.47, pp. 307-511, ISBN 0-12-007844-9

Hofstad, K.H.; Hoebink, J.H.B.J.; Holmen, A. & Marin, G.B. (1998). Partial oxidation of methane to synthesis gas over rhodium catalysts. *Catalysis Today,* Vol.40, No. 2-3, pp. 157-170, ISSN 0920-5861

Ishii, M.; Hayashi, T. & Matsumoto, S. (2002). Adsorption, desorption and decomposition of nitrogen monoxide on Rh(1 0 0) studied by electron-stimulated desorption, Auger electron spectroscopy and temperature-programmed desorption. *Applied Catalysis A: General*, Vol.225, No.1-2, pp. 207-213, ISSN 0926-860X

Kittel, Ch. (2005). *Introduction to Solid State Physics* John Willey & Sons. Inc, ISBN 0-471-41526-x, USA

Kraus, L.; Zaki, M.I.; Knözinger, H. & Tesche, B. (1989). Support and additive effects on the state of rhodium catalysts. *Journal of Molecular Catalysis*, Vol.55, No.1, pp. 55-69

Lavalley, J.C.; Saussey, J.; Lamotte, J.; Breault, R.; Hindennann, J.P. & Kiennemann, A. (1990). Infrared study of carbon monoxide hydrogenation over rhodium/ceria and rhodium/silica catalysts. *The Journal of Physical Chemistry*, Vol.94, No.15, pp. 5941–5947

Lide, D.R. (2004-2005). *Handbook of Chemistry and Physics*, CRC Press, ISBN 0-8493-0485-7, Boca Raton

Mallens, E. P. J.; Hoebink, J.H.B.J. & Marin, G.B. (1997). The reaction mechanism of the partial oxidation of methane to synthesis gas: A transient kinetic study over rhodium and a comparison with platinum. *Journal of Catalysis,* Vol.167, No.1, pp. 43-56, ISSN 0021-9517

Nakagawa, K.; Ikenaga, N.; Kobayashi, T. & Suzuki, T. (1999). Transient response of catalyst bed temperature in the pulsed reaction of partial oxidation of methane to synthesis gas over supported rhodium and iridium catalysts. *Journal of Catalysis,* Vol.186, No.2, pp. 405-413, ISSN 0021-9517

Papp, H. & Sabde, D.P. (2005). An investigation on the mechanism of NO decomposition over Rh/SiO_2 catalysts in presence of pulse injected H_2. *Applied Catalysis B: Environmental*, Vol.60, No.1-2, pp. 65-71, ISSN 0926-3373

Parvulescu, V.I.; Grange, P. & Delmon, B. (1998). Catalytic removal of NO. *Catalysis Today*, Vol.46, No.4, pp. 233-316, ISSN 0920-5861

Paul, D.K.; Marten, C.D. & Yates, J.T.Jr. (1999). Control of $Rh^{I}(CO)_2$ formation on Rh/Al_2O_3 catalysts by complexation of surface −OH groups using NH_3. *Langmuir*, Vol.15, No.13, pp. 4508–4512, ISSN 1520-5827

Pietraszek, A.; Da Costa, P.; Marques, R.; Kornelak, P.; Hansen, T.W.; Camra, J. & Najbar, M. (2007). The effect of the Rh–Al, Pt–Al and Pt–Rh–Al surface alloys on NO conversion to N_2 on alumina supported Rh, Pt and Pt–Rh catalysts. *Catalysis Today*, Vol.119, No.1-4, pp. 187-193, ISSN 0920-5861

Rahkamaa, K. & Salmi, T. (1999). Investigation of the catalytic decomposition of NO and N_2O on supported Rh with transient techniques. *Chemical Engineering Science*, Vol.54, No.20, pp. 4343-4349, ISSN 0009-2509

Rieck, J.S. & Bell, A.T. (1985). Studies of the interactions of H_2 and CO with silica- and lanthana-supported palladium. *Journal of Catalysis,* Vol.96, No.1, pp. 88-105, ISSN 0021-9517

Root, T.W.; Schmidt, L.D. & Fisher, G.B. (1983). Adsorption and reaction of nitric oxide and oxygen on Rh(111). *Surface Science*, Vol.134, No.1, pp. 30-45, ISSN 0039-6028

Sugisawa, T.; Shiraishi, J.; Machihara, D.; Irokawa, K.; Miki, H.; Kodama, C.; Kuriyama, T.; Kubo, T. & Nozoye, H. (2001). Adsorption and decomposition of NO on Pt (112). *Applied Surface Science*, Vol.169-170, pp. 292-295, ISSN 0169-4332

Thiam, M.M.; Hrčiř , T.; Matolin, V. & Nehasil, V. (2004). EELS and AES investigation of Rh thin film growth on polycrystalline Al substrate. *Vacuum*, Vol.74, No.2, pp. 141-145, ISSN 0042-207X

Tonetto, G.M.; Ferreira, M.L. & Damiani, D.E. (2003). A combined theoretical and experimental study of NO decomposition on Pd and Pd-Mo catalysts. *Journal of Molecular Catalysis A: Chemical*, Vol.193, No.1-2, pp. 121-137, ISSN 1381-1169

Wagner, Ch.D.; Naumkin, A.V.; Kraut-Vass, A.; Allison, J.W.; Powell, C.J. & Rumble, J.R.Jr. (2007). NIST X-ray Photoelectron Spectroscopy Database NIST Standard Reference Database 20, Version 3.5, Available from: http://srdata.nist.gov/xps/

Wang, D.; Dewaele, O.; Groote, A.M.D. & Froment, G.F. (1996). Reaction mechanism and role of the support in the partial oxidation of methane on Rh/Al_2O_3. *Journal of Catalysis*, Vol.159, No.2, pp. 418-426, ISSN 0021-9517

Wang, X.; Sigmon, S.M.; Spivey, J.J. & Lamb, H.H. (2004). Support and particle size effects on direct NO decomposition over platinum. *Catalysis Today*, Vol.96, No.1-2, pp. 11-20, ISSN 0920-5861

Yates, J.T.; Duncan, T.M.; Worley, S.D. & Vaughan, R.W. (1979). Infrared spectra of chemisorbed CO on Rh. *The Journal of Chemical Physics*, Vol.70, pp. 1219-1224, ISSN 1089-7690

Zimowska, M.; Wagner, J. B.; Dziedzic, J.; Camra, J.; Borzęcka-Prokop, B. & Najbar, M. (2006). Some aspects of metal-support strong interactions in Rh/Al_2O_3 catalyst under oxidising and reducing conditions. *Chemical Physics Letters,* Vol.417, No.1-3, pp.137-142, ISSN 0009-2614

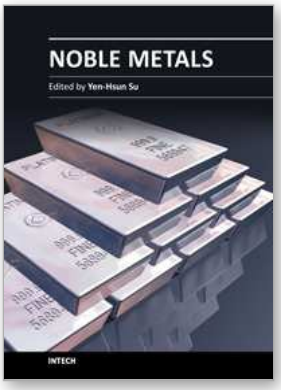

Noble Metals
Edited by Dr. Yen-Hsun Su

ISBN 978-953-307-898-4
Hard cover, 426 pages
Publisher InTech
Published online 01, February, 2012
Published in print edition February, 2012

This book provides a broad spectrum of insights into the optical principle, resource, fabrication, nanoscience, and nanotechnology of noble metal. It also looks at the advanced implementation of noble metal in the field of nanoscale materials, catalysts and biosystem. This book is ideal not only for scientific researchers but also as a reference for professionals in material science, engineering, nonascience and plasmonics.

How to reference
In order to correctly reference this scholarly work, feel free to copy and paste the following:

Patrick Da Costa, Jarosław Dutkiewicz, Valerio Choque, Narcis Homs, Paweł Kornelak, Mieczysława Najbar, Agnieszka Pietraszek, Pilar Ramirez de la Piscina and Janusz Sobczak (2012). Alloying Effect in Low Loaded Rh Catalysts Supported on High Surface Area Alumina on Their Activity in CH4 and NO Decomposition, Noble Metals, Dr. Yen-Hsun Su (Ed.), ISBN: 978-953-307-898-4, InTech, Available from: http://www.intechopen.com/books/noble-metals/alloying-effect-in-low-loaded-rh-catalysts-supported-on-high-surface-area-alumina-on-their-activity-

INTECH
open science | open minds

InTech Europe
University Campus STeP Ri
Slavka Krautzeka 83/A
51000 Rijeka, Croatia
Phone: +385 (51) 770 447
Fax: +385 (51) 686 166
www.intechopen.com

InTech China
Unit 405, Office Block, Hotel Equatorial Shanghai
No.65, Yan An Road (West), Shanghai, 200040, China
中国上海市延安西路65号上海国际贵都大饭店办公楼405单元
Phone: +86-21-62489820
Fax: +86-21-62489821